Precision Engineering 37 (2013) 531–541

Contents lists available at SciVerse ScienceDirect

Precision Engineering

journal homepage: www.elsevier.com/locate/precision

Incorporation of flexural hinge fatigue-life cycle criteria into the topological design of compliant small-scale devices

Frank Dirksen[a,b,*], Mathias Anselmann[a], Tarek I. Zohdi[b], Rolf Lammering[a]

[a] Institute of Mechanics, Helmut-Schmidt-University/University of the Federal Armed Forces Hamburg, Holstenhofweg 85, 22043 Hamburg, Germany
[b] Department of Mechanical Engineering, University of California, Berkeley, 6181 Etcheverry Hall, Berkeley, CA 94720, USA

ARTICLE INFO

Article history:
Received 13 December 2011
Received in revised form
24 November 2012
Accepted 16 December 2012
Available online 16 January 2013

Keywords:
Flexural hinges
Compliant mechanisms
Structural optimization
Fatigue life
Optimal design

ABSTRACT

The design synthesis of compliant mechanisms yields optimized topologies that combine several stiff parts with highly elastic flexural hinges. The hinges are often represented in a finite element analysis by a single node (one-node hinge), which leaves the actual physical meaning of the hinge (to be fabricated) ambiguous. In order to circumvent this problem, in this work, one-noded hinges have the fatigue-life incorporated into them during the design synthesis by embedding analytical expressions accounting for stress concentration, surface finish, non-zero mean stresses and superposed multiple loading conditions into the formulation. Various flexural hinges with rectangular, circular and parabolic profile geometries are investigated. By incorporating the hinge geometry and fatigue behavior into the design process, unclear interpretation issues that would be encountered during any later manufacturing stage of a compliant mechanism design are removed. Examples are provided to illustrate the overall process.

1. Introduction

In order to create machine tools for small-scale applications, compliant mechanisms (CM) have become quite popular in recent years, as an alternative to rigid body systems connected by conventional pin joints. CM are flexible, monolithic structures whose overall motion is a result of the (elastic) deformation of certain components, so-called flexural hinges. CM are potentially more accurate, have superior scalability, cleaner, less noisy and, most importantly, less expensive to manufacture and maintain than conventional devices. However, there are two major drawbacks: (1) designing CM is more difficult and nonintuitive, due to its inherent complex overall deformation and (2) fatigue effects on the flexural hinges can lead to premature failure of the entire CM under dynamic loading conditions.

Several approaches have arisen to address the first issue by applying numerical topology design and optimization procedures. Relevant contributions have been made by various research teams, e.g. [1–7]. All these techniques lead, in a systematic manner, to final optimized topologies, i.e., an optimal distribution of material over the design domain is obtained to meet the user-specified motion requirements. As a key result, one-noded hinges (often called pseudo-hinges) arise, which have a physically unclear interpretation. Although some techniques exist for circumventing this critical issue, e.g. [8], in this work, we propose to circumvent this problem, by having one-noded hinges with the fatigue-life incorporated into them during the design synthesis by embedding analytical expressions accounting for stress concentration, surface finish, non-zero mean stresses and superposed multiple loading conditions into the formulation. This is achieved by utilizing data from the finite element calculations during the topology optimization process. Since nodal displacements for a given topology are known, the required deflection ranges and (internal) nodal forces are already available, without additional cost. This information can be used to replace one-node hinges with real flexural hinges that meet the deflection and fatigue requirements, dependent on their specific geometry and material.

The mechanical properties of flexural hinges under static loading have been investigated previously. Paros and Weisbord did pioneering work, yielding the approximate compliances of flexural hinges [9]. Background information on flexural elements and systems can be found in Smith [10]. Lobontiu et al. and Tian et al. analytically investigated flexural hinges based on energy principles to calculate the desired properties at individual points within hinges [11,12] and proposed valuable closed-form equations of differently shaped flexure hinges

* Corresponding author: Institute of Mechanics, Helmut-Schmidt-University/University of the Federal Armed Forces Hamburg, Holstenhofweg 85, 22043 Hamburg, Germany. Tel.: +49 40 6541 2745; fax: +49 40 6541 2034.
E-mail address: frank.dirksen@cal.berkeley.edu (F. Dirksen).

0141-6359/$ – see front matter © 2013 Elsevier Inc. All rights reserved.
http://dx.doi.org/10.1016/j.precisioneng.2012.12.005

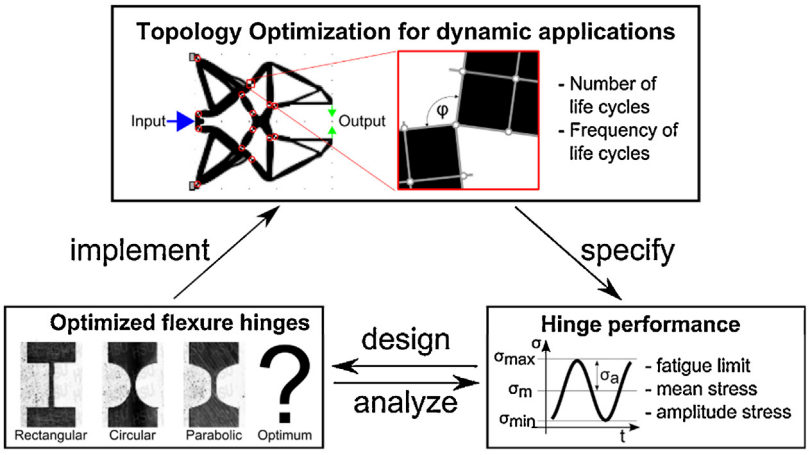

Fig. 1. Synthesis of compliant mechanisms: replacing artificial one-noded hinges by appropriate flexural hinge types meeting specified, known hinge requirements.

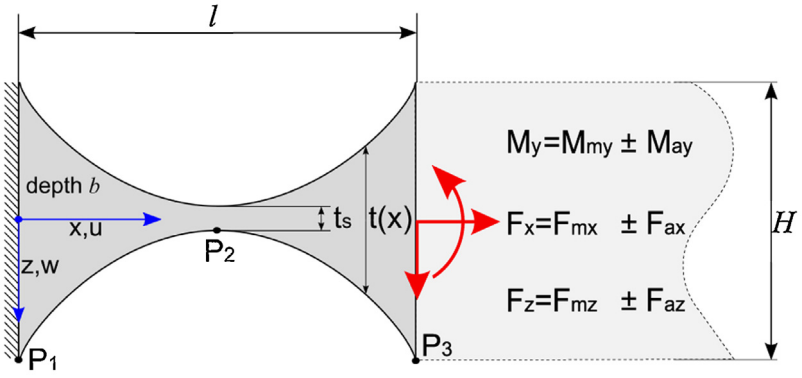

Fig. 2. Planar, flexural hinge characterized by length l, depth b, height H, variable thickness $t(x) \geq t_s$ and common points P_1, P_2, P_3 to resist external (nodal) loads F_x, F_z, M_y.

[13,14]. Recently, mechanical properties of flexural hinges were derived and validated, providing a guide from a topology optimization standpoint, for static loading conditions [15].

In spite of the cited research, the fatigue life of flexural hinges in compliant mechanisms has not been fully analyzed yet, and, to the author's knowledge, there are too little of experimental data as pointed out rightly in a fairly recent review paper [16]. In terms of the synthesis of compliant mechanisms, this leaves a gap between final, optimized topologies and appropriate flexural hinges that meet (or exceed) a desired number of life cycles. In order to bridge this gap, fatigue limits for flexural hinges are derived and applied in this work to provide a guide of designing flexural hinges for dynamic applications from a topology optimization standpoint, prior to any modelling and manufacturing efforts. The overall scheme is shown in Fig. 1.

2. Objectives

For the synthesis of compliant mechanisms for dynamic applications, it is crucial to know the fatigue limit of embedded flexural hinges. Assuming harmonic loading with constant amplitudes, explicit analytical expressions of fatigue limits, based on the geometric shape and material of flexural hinges are derived, using a standard x–z-coordinate system, as shown in Fig. 2, by applying different established theories and models. These explicit expressions are then (inversely) solved to design appropriate flexural hinges with infinite life based on specified loads.

In this work, planar flexural hinges of different geometries are examined. Specifically, rectangular, circular and parabolic flexural hinges, denoted by superscripts R, C, P respectively, are investigated due to their easy manufacturability and convenient mathematical handling.[1]

The geometry of flexural hinges is described by length l, height H and variable thickness $t(x) \geq t_s$, as well as common points $P_1(0, H/2)$, $P_2(l/2, t_s/2)$ and $P_3(l, H/2)$, as shown in Fig. 2. The depth is set to uniform $b = 10$ mm over the entire hinge, which is sufficient for the majority of planar applications.

The key aspect for the following calculations is the geometric shape, given by the variable thickness $t(x)$ of each type of flexural hinge

$$t^R(x) = t_s, \tag{1}$$

$$t^P(x) = 2(c_1 + c_2 x + c_3 x^2) = H - \frac{4(H - t_s)}{l} x + \frac{4(H - t_s)}{l^2} x^2, \tag{2}$$

[1] Circular shapes are approximated by parabolic functions using Taylor expansion to avoid complicated expressions. The geometric approximation error was checked and is negligible in all loaded regions.

Table 1
Material properties of aluminum alloys mainly used in compliant mechanisms [17].

Name	E (GPa)	$S_{0.2}$ (MPa)	S_U (MPa)	ε_{max}
Al 2024-O	73	75	185	20%
Al 2024-T3	73	345	485	18%
Al 2024-T351	73	325	470	20%

$$t^C(x) = 2\left(z_M + \sqrt{r^2 - (x - x_M)^2}\right) = \frac{H^2 - t_s^2 + l^2}{4(H - t_s)} - \sqrt{\frac{\left(l^2 + (H - t_s)^2\right)^2}{(4(H - t_s))^2} - \frac{(l - 2x)^2}{4}}. \tag{3}$$

Parabolic and circular hinges are first written in a general form denoted by polynomial coefficients c_1, c_2, c_3 and circle's center coordinates x_M, z_M and radius r, respectively. In the second line of Eqs. (2) and (3), relevant geometric boundary conditions

$$\begin{aligned} c_1 &= \frac{H}{2}, \quad c_2 = \frac{-2(H - t_s)}{l}, \quad c_3 = \frac{2(H - t_s)}{l^2}, \\ x_M &= \frac{l}{2}, \quad z_M = \frac{t_s}{2} + r, \qquad r = \frac{l^2 + (H - t_s)^2}{4(H - t_s)}, \end{aligned} \tag{4}$$

are applied. Throughout this paper, the formulations $t^{R,P,C} = t^{R,P,C}(x, H, l, t_s)$ are used to keep the solution general and adaptable.

In order to compare analytical results with numerical and experimental data, high strength Aluminum wrought alloys, which are often used in applications of CM due to their high fatigue strength and elastic properties, are considered throughout this work. The relevant material specifications are listed in Table 1.

3. Stresses in flexural hinges

Since flexural hinges are mainly used in CM to allow rotational motion, the main focus is on axial bending caused by the external nodal forces F_x, F_z and the moment $M_y(x)$, as illustrated in Fig. 2. All loads are assumed to be time-harmonic, with constant mean and amplitude, denoted by index m and index a, respectively. For example, $M_y = M_{my} \pm M_{ay}$ causes time-harmonic (bending) stresses $\sigma_b = \sigma_{mb} \pm \sigma_{ab}$, as illustrated in Fig. 1.

3.1. Moments of area

The moments of area for the considered flexural hinges are required to calculate the stresses in the following sections. The areas of the cross-section are

$$A^{R,P,C}(x) = bt^{R,P,C}(x), \tag{5}$$

and the second moments of area $I_y(x)$ are

$$\begin{aligned} I_y^R &= \frac{bt_s^3}{12}, \\ I_y^P(x) &= \frac{b(H(l - 2x)^2 + 4t_s(l - x)x)^3}{12l^6}, \\ I_y^C(x) &= \frac{b((x - x_M)^2 + 2r(z_M - r))^3}{12r^3}, \end{aligned} \tag{6}$$

where the thicknesses t_s and $t^{R,P,C}(x)$ are given in Eqs. (1)–(3). The listed moments of area are used to calculate nominal stresses in the upcoming section.

3.2. Nominal stresses σ_a, σ_m

The largest principal tensile stress is the most significant stress component in fatigue analysis for the materials typically used in CM [18]. Assuming negligible normal stresses in lateral direction, i.e., $\sigma_y = \sigma_z = 0$, this equals the normal stress in the x-direction $\sigma_x(x, z) = (F_x/A(x)) + (M_y(x)/I_y(x))z$, which depends on the external loads, cross-section $A(x)$, depth b, second area moment $I_y(x, z)$ and the z-coordinate, where a linear-elastic, isotropic stress–strain relation is assumed. Thus, the relevant nominal stresses within flexural hinges are

$$\begin{aligned} \sigma_x^R(z) &= \frac{1}{bt_s}F_x + \frac{12(x - l)z}{bt_s^3}F_z + \frac{12z}{bt_s^3}M_y, \\ \sigma_x^P(x, z) &= \frac{l^2}{bh_*^3(x)}F_x + \frac{12l^6 z}{bh_*^9(x)}M_y + \frac{12l^6(x - l)z}{bh_*^9(x)}F_z, \\ \sigma_x^C(x, z) &= \frac{1}{2bh_{**}(x)}F_x + \frac{3z(x - l)}{2bh_{**}(x)}M_y + \frac{3z}{2bh_{**}(x)}F_z, \end{aligned} \tag{7}$$

where $h_*^3(x) = H(l - 2x)^2 + 4(l - x)xt_s$ and $h_{**}(x) = z_M - \sqrt{r^2 - (x - x_M)^2}$ are introduced to keep the expressions concise.

Table 2
Fatigue strengths (S_f) in absence of mean stresses ($\sigma_m = 0$): experimental data $S_{f,\exp}$ [17], a linear estimate [18], bending fatigue strength $S_{fb,Ra}$ and tensile fatigue strength $S_{ft,Ra}$ [19].

Name	$S_{f,\exp}$ (MPa)	$S_{ft} = \alpha S_U$ (MPa)	$S_{fb,R}$ (MPa)	$S_{ft,R}$ (MPa)
Al 2024-O	90	65	74	63
Al 2024-T3	140	170	130	111
Al 2024-T351	140	165	130	111

In the ensuing sections, the axial force F_x causes a tensile stress σ_t whereas the moment M_y and the force F_z cause a bending stress, σ_b, within the cross-section of the flexural hinges. For both loading conditions, the resulting mean stresses $\sigma_m = (\sigma_{\max} + \sigma_{\min})/2$, amplitude stresses $\sigma_a = (\sigma_{\max} - \sigma_{\min})/2$ and ratio $R = \sigma_{\min}/\sigma_{\max}$ can be calculated using the nominal stresses $\sigma^{R,P,C}_{x,\max}$ which occur at the thinnest cross section at the upper or lower edge substituting ($x = l/2$) and $z = \pm t_s/2$ into Eq. (7).

4. Fatigue strength of flexural hinges

The fatigue strengths of different flexural hinges are calculated using the stress-life approach. Accordingly, first, the fatigue strength of a smooth test specimen is determined. This value is then lowered by applying different reduction factors ("knock-down factors") which account for nonzero mean stresses, notch effects and surface finish. Thermal effects (both ambient and generated) are considered negligible for the applications of interest.

4.1. Fatigue strength with no mean stress ($\sigma_m = 0$)

Fatigue strengths have been determined by extensive experiments and, thus, are known for some materials. However, if bending fatigue strength S_{fb} and tensile fatigue strength S_{ft} are not available, they can be estimated in absence of mean stress ($\sigma_m = 0$) based on numerous experiments on unnotched standard test pieces. There are different methods to estimate the fatigue strengths. A classical approach is given by using the linear relation between tensile fatigue strength S_{ft} and ultimate tensile strength S_U

$$S_{ft} = \alpha S_U, \tag{8}$$

where the factors $\alpha = 0.5$ for steel and Titanium alloys, and $\alpha = 0.35$ for Aluminum alloys are typically used. As mentioned in [18], this is not necessarily a good measure and only provides an initial estimate. Another approach was used by Radaj and Vormwald [19], where the bending fatigue strength $S_{fb,Ra}$ was estimated for Aluminum alloys possessing different tensile strengths for $N = 10^8$ life cycles by the following

$$S_{fb,R} \approx \begin{cases} 0.4 S_U & \text{for } S_U \le 325\,\text{MPa} \\ 130\,\text{MPa} & \text{for } S_U \ge 325\,\text{MPa} \end{cases}, \tag{9}$$

and the tensile fatigue strengths $S_{ft,Ra}$ were further reduced to

$$S_{ft,Ra} \approx 0.85\, S_{fb,R}. \tag{10}$$

The different fatigue strengths in absence of any mean stresses ($\sigma_m = 0$) are listed in Table 2. Index i is used for formulas which apply to both, tensile and bending load. Otherwise the indexes b for bending and t for tension are used separately.

4.2. Fatigue strength with nonzero mean stress ($\sigma_m \neq 0$)

Considering nonzero mean stresses, the maximum permissible stress amplitudes need to be formulated as a function of the mean stresses $S_{ai}(\sigma_m)$, i.e., the same number of life cycles can only be achieved for higher mean stresses σ_m by reducing the stress amplitudes σ_a. Three classical relations have been proposed by Gerber [20], Goodman [21] and Soderberg [22], respectively:

$$\text{Gerber}: \quad S_{ai}(\sigma_m) = S_{fi}\left(1 - \left(\frac{\sigma_m}{S_U}\right)^2\right), \tag{11}$$

$$\text{Mod.Goodman}: \quad S_{ai}(\sigma_m) = S_{fi}\left(1 - \frac{\sigma_m}{S_U}\right), \tag{12}$$

$$\text{Soderberg}: \quad S_{ai}(\sigma_m) = S_{fi}\left(1 - \frac{\sigma_m}{S_{0.2}}\right), \tag{13}$$

as illustrated in Fig. 3(a). Soderberg provides a very conservative estimate, whereas Goodman and Gerber match experimental data quite well [23]. The modified Goodman relation is used in this work.

4.3. Notch effect

The fatigue strength of a flexural hinge is significantly lower than it is for unnotched test specimen, due to stress concentrations that occur at the root of flexural hinge, causing nucleation of microcracks which possibly leads to failure. In a quasi-static analysis, the stress concentration factor K_{ti} is mainly used to account for the occurring higher peak stresses, compared to the nominal stresses, as shown in

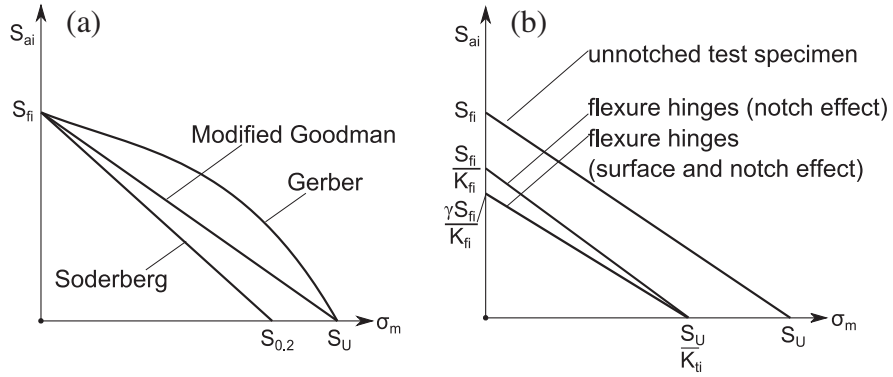

Fig. 3. Fatigue diagrams: (a) three established relations and (b) reduced fatigue strength of flexural hinges using modified Goodman relation.

[15]. The stress concentration factors for rectangular leaf type hinges strongly depends on the corner radius and can be found in [24]. For circular and parabolic hinges, stress concentration factors for tension $K_{tt}^{C,P}$ and bending $K_{tb}^{C,P}$ can be approximated following [25,26]

$$K_{tt}^{C,P} = 1 + \left[0.1\left(\frac{r}{t^*}\right) + 0.7\left(1+\frac{t_s}{2r}\right)^2\left(\frac{t_s}{2r}\right)^{-3} + 0.13\left(\frac{t_s}{2r}\right)\left(\frac{t_s}{2r}+\frac{t^*}{r}\right)^{-1}\left(\frac{t^*}{r}\right)^{-1.25}\right]^{-(1/2)},$$
$$K_{tb}^{C,P} = 1 + \left[0.08\left(\frac{r}{t^*}\right)^{0.66} + 2.2\left(1+\frac{t_s}{2r}\right)^{2.25}\left(\frac{t_s}{2r}\right)^{-3.375} + 0.2\left(\frac{t_s}{2r}\right)\left(\frac{t_s}{2r}+\frac{t^*}{r}\right)^{-1}\left(\frac{t}{r}\right)^{-1.33}\right]^{-(1/2)}, \quad (14)$$

where $t^* = ((H - t_s)/2)$ and the radii of curvature r are

$$r^C = \frac{l^2 + (H-t_s)^2}{4(H-t_s)} = const. \quad (15)$$

and

$$r^P\left(x = \frac{l}{2}\right) = \frac{l^2}{4(H-t_s)}, \quad (16)$$

for circular and parabolic hinges as shown in Fig. 4. Here, the geometric properties given in Eq. (2) and corresponding derivatives $t'(x)$, $t''(x)$ were applied to calculate the radius of curvature of a parabola

$$r^P(x) = \left|\frac{(1+t'(x)^2)^{3/2}}{t''(x)}\right|.$$

In fatigue analysis, various experiments have suggested that the (static) stress concentration factor overestimates the notch severity of flexural hinges. Therefore, the "notch effect" is described more accurately by the fatigue strength reduction factor K_{fi}, also called fatigue

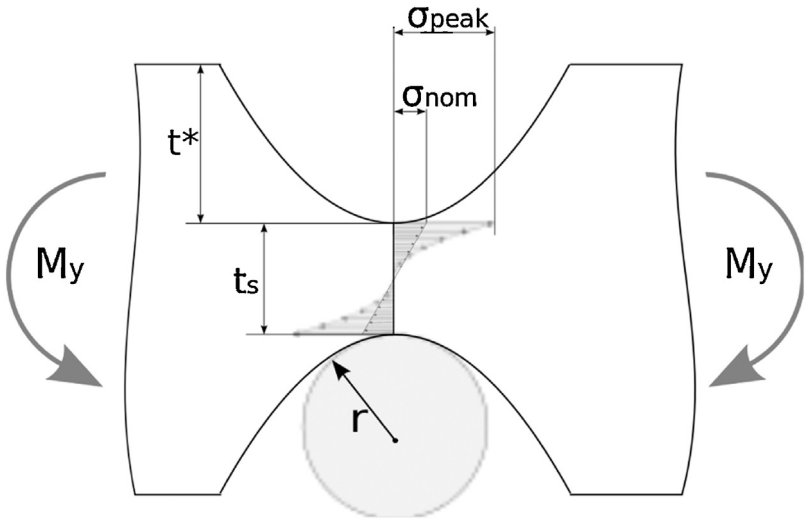

Fig. 4. Peak stresses depending on the curvature at the root lead to a reduced fatigue strength of flexural hinge.

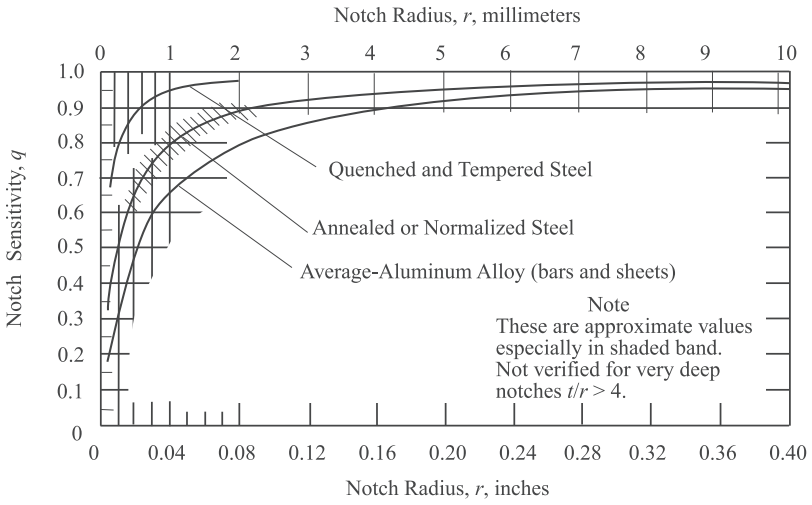

Fig. 5. Notch sensitivity for different radii r [24].

notch factor, defined as the ratio of the fatigue strength of unnotched test specimen (as described in the previous section) and the fatigue strength of the notched specimen, i.e., the flexural hinge:

$$1 \le K_{fi} = \frac{S_{fi,Test\ Specimen}}{S_{fi,Flexure\ Hinge}} \le K_{ti}. \tag{17}$$

The fatigue strength reduction factor K_{fi} can be calculated using the notch sensitivity q, which is defined as

$$q = \frac{K_{fi} - 1}{K_{ti} - 1}, \tag{18}$$

where q varies from zero (no notch effect: $K_{fi} = 1$) to one (full notch effect $K_{fi} = K_{ti}$) and can be determined from Fig. 5.

K_{fi} can also be determined from experiments or empirical measures as proposed by Peterson or Neuber:

$$\text{Peterson}: \quad K_{fi} = 1 + \frac{K_{ti} - 1}{1 + (A_P/r)}, \tag{19}$$

$$\text{Neuber}: \quad K_{fi} = 1 + \frac{K_{ti} - 1}{1 + \sqrt{A_N/r}}, \tag{20}$$

with A_P and A_N as material constants depending on the strength and ductility, e.g., $A_P \approx 0.66$ for Aluminum alloys [27]. Thus, the reduced fatigue strength of flexural hinges is calculated by Eqs. (11)–(13) yielding, for example, following Goodman

$$S_{ai}(\sigma_m) = \frac{S_{fi}}{K_{fi}} \left(1 - \frac{\sigma_m}{S_U/K_{ti}}\right), \tag{21}$$

as illustrated in Fig. 3(b) where the ordinate and abscissa are scaled by $1/K_{ti}$ and $1/K_{fi}$, respectively.

4.4. Superposed bending and tension

Thus far, pure bending or pure tensile cyclic loads was considered. Although superposed bending and tension cause similar critical stresses, the overall fatigue life is unequally more complex due to different amplitudes, frequencies and phase relations. There are, to the authors' knowledge, neither material parameters nor precise methods known that hold for arbitrary loading conditions. However, a reasonable equivalent stress $\sigma_{a,e}$ can be estimated following Issler et al. [27] by choosing, for example, the tensile loading as a reference yielding

$$\sigma_{a,e} = \sigma_{at} + \kappa\sigma_{ab}, \tag{22}$$

with $\kappa = S_{at}/S_{ab}$ as a reference coefficient.

4.5. Surface effect

The surface roughness of the root of flexural hinges affects the fatigue strength significantly, due to possible crack nucleation and propagation on the surface. The surface roughness reduction factor γ accounts for different surface qualities obtained by different manufacturing technologies, such as polishing, grinding, milling, and drilling. It is defined as the ratio of the fatigue strength of standard test specimen with a specific surface quality and the fatigue strength of a very smooth test specimen

$$\gamma = \frac{S_{fi}}{S_{fi,smooth}}. \tag{23}$$

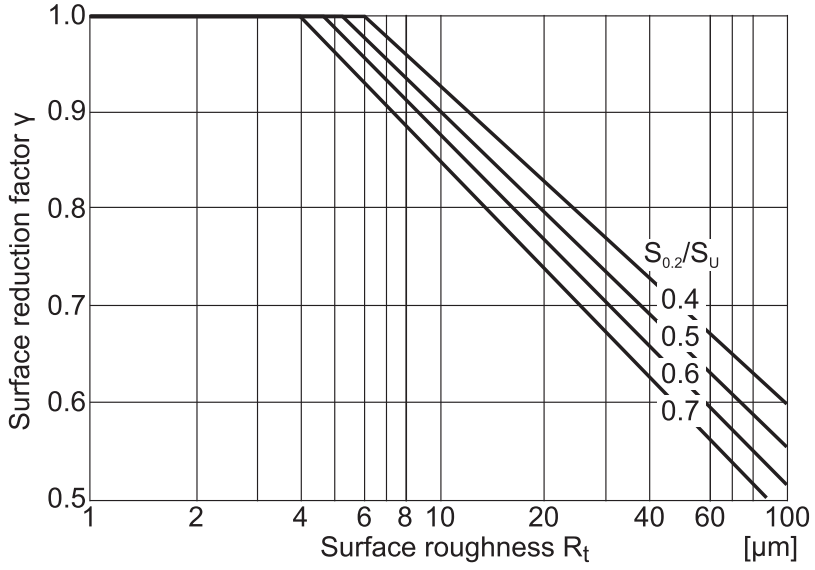

Fig. 6. Surface roughness reduction factor γ for Al wrought alloys adopted and modified from [19] based on VDI guideline 2226 [28].

It is assumed that the influence of the surface finish is similar for unnotched and notched test specimens. Therefore, values for γ, which were measured on unnotched test specimen are applied to flexural hinges, as well. The surface reduction factor γ depending on the surface roughness R_t, also called total height of the profile, is shown in Fig. 6.

The absolute arithmetic *average* surface roughness R_a for electric discharged machined specimens is typically within a range of 1.6–5 μm [29]. There is no mathematical relation between R_t and R_a. However, an experience-based estimate is given in [30] by a factor of 8.7 yielding approximate values of $R_t \approx 14$–44 μm. Assuming a reasonable surface roughness of $R_t \approx 20$ μm yields for Al wrought alloys mainly used in CM, e.g., Al 2024-T3 or Al 2024-T351, with a ratio $S_{0.2}/S_U \approx 0.7$ a surface reduction factor of $\gamma = 0.75$.

The fatigue strength of flexural hinges is further reduced to

$$S_{ai}(\sigma_m) = \frac{S_{fi}}{K_{fi}} \left(1 - \frac{\sigma_m}{S_U/K_{ti}}\right), \tag{24}$$

as illustrated in Fig. 3(b) where the ordinate and abscissa are further scaled by γ.

Generally, the resulting fatigue strength of flexural hinges depend on the surface finish and on notch effect that is linked directly with the radii of curvature, i.e., smaller radii of curvature result in lower fatigue strengths. This is not a surprising result, however Eqs. (14)–(24) provide explicit analytical expressions to calculate the reduced fatigue strength of flexural hinges prior to any modeling or manufacturing efforts.

4.6. Fatigue safety factor

The resulting mean and amplitude stresses σ_m, σ_a that occur in flexural hinges can be calculated by Eq. (7) based on given loads, for example, from the topological synthesis. The highest capable stress amplitude for a given mean stress $S_{ai}(\sigma_m)$ is linked to the flexural hinges geometric and material properties by Eq. (24). The ratio of these values is typically referred as the safety factor S_D as

$$S_D = \frac{S_{at}(\sigma_m)}{\sigma_{a,e}}, \tag{25}$$

with $\sigma_{a,e}$ as defined in Eq. (22).

5. Design of optimal flexural hinges

The optimal shape of circular and parabolic flexural hinges are calculated inversely based on the explicit expressions derived in the previous section and linked to the safety factor S_D. In any case, the maximum mean and amplitude stresses depend on the given loads as written in Eq. (7) and occur at $x = (l/2)$ and $z = \pm(t_s/2)$:

$$\begin{aligned} \sigma_{mb} &= \frac{6}{bt_s^2} M_{my} - \frac{3l}{bt_s^3} F_{mz}, & \sigma_{ab} &= \frac{6}{bt_s^2} M_{ay} - \frac{3l}{bt_s^3} F_{az}, \\ \sigma_{mt} &= \frac{1}{bt_s} F_{mx}, & \sigma_{at} &= \frac{1}{bt_s} F_{ax}. \end{aligned} \tag{26}$$

Remark. The hinge height H is substituted by the relation $H = 2t^* + t_s$ as illustrated in Fig. 4.

5.1. Circular flexural hinges

In order to connect the geometric properties of circular flexural hinges to the safety factor, the stress concentration factors are obtained by Eqs. (14) and (15):

$$K_{tb}^{C} = 1 + \left(\frac{0.32}{(4 + (l^2/t^{*2}))^{0.66}} + \frac{0.01(l^2 + 4t^{*2})^{1.33} t_s}{t^{2.66}(2t^* + t_s)} + \frac{0.02(l^2 + 4t^{*2})^{1.13}(l^2 + 4t^*(t^* + t_s))^{2.25}}{(t^* t_s)^{3.375}} \right)^{-0.5}, \tag{27}$$

$$K_{tt}^{C} = 1 + \left(0.01 + \frac{0.013 l^2}{t^2} + \frac{0.01(l^2 + 4t^{*2})^{1.25} t_s}{t^{2.5}(2t^* + t_s)} + \frac{0.01(l^2 + 4t^{*2})(l^2 + t^*(4t^* + 4t_s))^2}{t^{*3} t_s^3} \right)^{-0.5}. \tag{28}$$

The fatigue strengths become with Eqs. (15), (19), (24) and (26)

$$\begin{aligned} S_{ab} &= \frac{S_{fb}(l^2 + 4t^*(2A_P + t^*))(3F_{mz}K_{tb}^{C} l - 6K_{tb}^{C} M_{my} + bS_U t_s^2)\gamma}{bS_U(8A_P t + K_{tb}^{C}(l^2 + 4t^{*2}))t_s^2}, \\ S_{at} &= \frac{S_{ft}(l^2 + 4t^*(2A_P + t^*))(-F_{mx}K_{tt}^{C} + bS_U t_s)\gamma}{bS_U(8A_P t^* + K_{tt}^{C}(l^2 + 4t^2))t_s}. \end{aligned} \tag{29}$$

Substituting Eq. (29) into Eq. (22) yield the equivalent stress

$$\begin{aligned} \kappa &= \frac{S_{ft}(8A_P t^* + K_{tb}^{C}(l^2 + 4t^{*2}))t_s(-F_{mx}K_{tt}^{C} + bS_U t_s)}{S_{fb}(8A_P t^* + K_{tt}^{C}(l^2 + 4t^{*2}))(3F_{mz}K_{tb}^{C} l - 6K_{tb}^{C} M_{my} + bS_U t_s^2)}, \\ \sigma_{a,e} &= \frac{1}{bt_s} F_{ax} + \kappa \left(\frac{6}{bt_s^2} M_{ay} - \frac{3l}{bt_s^3} F_{az} \right). \end{aligned} \tag{30}$$

The safety factor becomes after substituting Eqs. (27)–(30) into Eq. (25):

$$S_D = \frac{\gamma S_{fb} S_{ft}(l^2 + 4t^*(2A_p + t^*)(-F_{mx}K_{tt}^{C} + bS_U t_s)(3F_{mz}K_{tb}^{C} l - 6K_{tb}^{C} M_{my} + bS_U {t_s}^2)}{(3S_U S_{ft}(F_{az} l - 2M_{ay})(8A_P t^* + K_{tb}^{C}(l^2 + 4t^{*2}))(F_{mx}K_{tt}^{C} - bS_U t_s) + F_{ax} S_{fb}(8A_P t^* + K_{tt}^{C}(l^2 + 4t^{*2}))(3F_{mz}K_{tb}^{C} l - 6K_{tb}^{C} M_{my} + bS_U {t_s}^2))} \tag{31}$$

This expression explicitly links the safety factor S_D with the design variables of the circular flexural hinge, i.e., the thicknesses t_S, t^* and the length l.

Remark. The relevant variables are printed in bold and the dependencies, e.g., $K_{tt} = K_{tt}(t_s, t^*)$, are omitted for simplicity.

5.2. Parabolic flexural hinges

In order to connect the geometric properties of parabolic flexural hinges to the safety factor, the stress concentration factors are obtained by Eqs. (14) and (16)

$$K_{tb}^{P} = 1 + \left(\frac{0.32 t^{*1.32}}{l^{1.32}} + \frac{0.01 l^{2.66} t_s}{t^{*2.66}(2t^* + t_s)} + \frac{0.02(l^3 + 4lt^* t_s)^{2.25}}{(t^* t_s)^{3.375}} \right)^{-0.5}, \tag{32}$$

$$K_{tt}^{P} = 1 + 3.67 \left(\frac{1}{t^{*5.5} t_s^3 (2.t^* + t_s)} l^{2.5} \left(0.29(lt^*)^{3.5} + 0.15 l^{3.5} t^{*2.5} t_s + 0.13 t^{*3} t_s^4 + l^{1.5} t_s (2.35 t^{*4.5} + 1.18 t^{*3.5} t_s) + \frac{t_s^2 (4.71 t^{*5.5} + 2.69 t^{*4.5} t_s + 0.17 t^{*3.5} t_s^2)}{l^{0.5}} \right) \right)^{-0.5}. \tag{33}$$

The fatigue strengths become with Eqs. (16), (19), (24) and (26)

$$\begin{aligned} S_{ab} &= \frac{\gamma(l^2 + 8t^* A_P) S_{fb}(3l F_{mz} K_{tb}^{P} - 6K_{tb}^{P} M_{my} + bS_U t_s^2)}{b(8t^* A_P + l^2 K_{tb}^{P}) S_U t_s^2}, \\ S_{at} &= \frac{\gamma(l^2 + 8t^* A_P) S_{ft}(-F_{mx}K_{tt}^{P} + bS_U t_s)}{b(8t^* A_P + l^2 K_{tt}^{P}) S_U t_s}. \end{aligned} \tag{34}$$

The equivalent stress $\sigma_{a,e}$ becomes with Eq. (22):

$$\begin{aligned} \kappa &= \frac{(8t^* A_P + l^2 K_{tb}^{P}) S_{ft} t_s(-F_{mx}K_{tt}^{P} + bS_U t_s)}{(8t^* A_P + l^2 K_{tt}^{P}) S_{fb}(3K_{tb}^{P}(lF_{mz} - 2M_{my}) + bS_U t_s^2)}, \\ \sigma_{a,e} &= \frac{1}{bt_s} F_{ax} + \kappa \left(\frac{6}{bt_s^2} M_{ay} - \frac{3l}{bt_s^3} F_{az} \right). \end{aligned} \tag{35}$$

The safety factor becomes after substituting Eqs. (32)–(35) into Eq. (25):

$$S_D = \frac{\gamma S_{fb} S_{ft} t_s^2 (l^2 + 8t^* A_P)(-F_{mx}K_{tt}^{P} + bS_U t_s)(3K_{tb}^{P}(lF_{mz} - 2M_{my}) + bS_U t_s^2)}{S_U t_s (3F_{x,a} t_s K_{t_b}^{P}(8t^* A_P + l^2 K_{tt}^{P})(lF_{mz} - 2M_{my}) S_{fb} + 3(F_{az} l - 2M_{ay}) F_{mx}(8t^* A_P + l^2 K_{tb}^{P}) K_{tt}^{P} S_{ft} t_s + bS_U t_s^2 (F_{ax} t_s (8t^* A_P + l^2 K_{tt}^{P}) S_{fb} - 3S_{ft}(F_{az} l - 2M_{ay})(8t^* A_P + l^2 K_{tb}^{P})))}. \tag{36}$$

This expression links explicitly the safety factor S_D with the design variables of the parabolic flexural hinge, i.e., the thicknesses t_S, t^* and the length l.

Remark. Again, the relevant variables are printed in bold and the dependencies, e.g., $K_{tt} = K_{tt}(t_s, t^*)$, are omitted for simplicity.

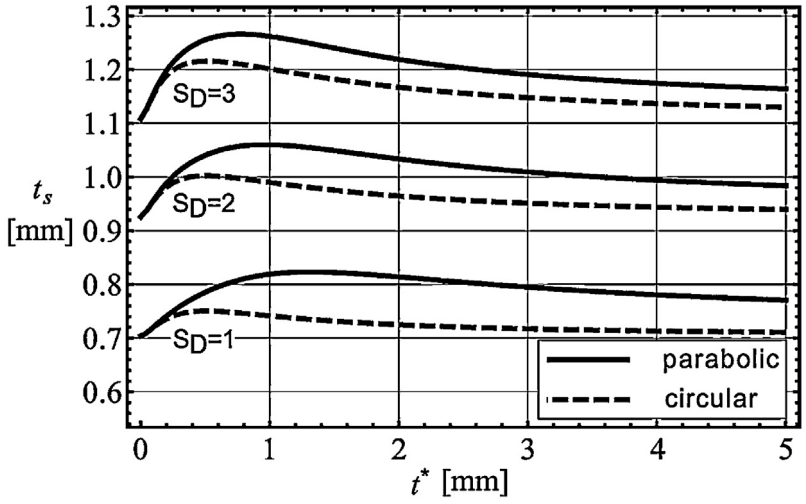

Fig. 7. Safety factor S_D as a function of t^* and t_s for parabolic and circular flexural hinges (see Example 2).

5.3. Geometrical parameter selection

Eqs. (31) and (36) are nonlinear functions $S_D(t^*, t_s, l)$, where t^*, t_s and l must to meet given geometric specifications. Maximizing $S_D(t^*, t_s, l)$ results in a flexural hinge with optimal geometric properties. In general, this problem can be solved numerically. However, plotting $S_D(t^*, t_s, l)$ as given in Eqs. (31) and (36) is not very costly and enables the analyst to easily pick optimal geometric parameters for different safety factors. An example is given in Fig. 7 and discussed in Section 6.2. It can be seen, that circular hinges yield higher safety factors than parabolic hinges, for a given thinnest cross-section t_S, i.e., an infinite life is more likely using circular hinges. In other words, circular hinges can have a thinner cross-section than parabolic hinges for a given safety factor. However, the reader should be aware that circular flexural hinges are not necessarily the best choice in terms of deflection range and precision, as described [15].

6. Examples on analysis and optimal design

6.1. Example 1: life cycle analysis of a flexural hinge undergoing superposed bending and tension

Consider a given parabolic flexural hinge ($H = 10$ mm, $l = 8$ mm, $b = 10$ mm, $t_s = 0.5$ mm) is undergoing a cyclic loading of $M_y = 20 \pm 30$ N mm^{-1} and $F_x = 10 \pm 20$ N. The monolithic CM is made of Al wrought alloy T3 and the hinges are manufactured by wire cutting-EDM (surface roughness $R_t = 20$ μm). A check is made for infinite life (with a safety factor $S_D \geq 2$) by performing the following:

1. Calculate the maximum nominal stresses by Eq. (7):

$$\sigma_{mb} = \frac{6}{bt_s^2} M_{my} = 48\ \text{N mm}^{-2}, \quad \sigma_{ab} = \frac{6}{bt_s^2} M_{ay} = 72\ \text{N mm}^{-2},$$
$$\sigma_{mt} = \frac{1}{bt_s} F_{mx} = 2\ \text{N mm}^{-2}, \qquad \sigma_{at} = \frac{1}{bt_s} F_{ax} = 4\ \text{N mm}^{-2}.$$

2. Determine the ultimate tensile strength and the fatigue strength of unnotched test specimen from Tables 1 and 2:

$$S_U = 485\ \text{MPa}, \quad S_{fb,R} = 130\ \text{MPa}, \quad S_{ft,R} = 111\ \text{MPa}.$$

3. Calculate the fatigue strength reduction factor by Eq. (19) using Eqs. (14) and (16):

$$r = 1.68\ \text{mm}, \quad K_{tb} = 1.02, \quad K_{tt} = 1.06, \quad K_{fb} = 1.01, \quad K_{ft} = 1.04.$$

4. Determine the surface roughness reduction factor by Fig. 6:

$$\gamma = 0.75.$$

5. Calculate the fatigue strength of the flexural hinge by Eq. (24) using the results from steps 2 to 4:

$$S_{ab} = 86.78\ \text{MPa}, \quad S_{at} = 79.73\ \text{MPa}.$$

6. Calculate the equivalent deflection stress σ_{ae} by Eq. (22):

$$\kappa = 0.92, \quad \sigma_{ae} = 70.2\ \text{N mm}^{-2}.$$

7. Calculate the safety factor using Eq. (25) and check with specifications:

$$S_D = 1.14 < 2.$$

Conclusion: Reliability of the parabolic flexural hinge against fatigue failure with a safety factor $S_D \geq 2$ cannot be guaranteed. A logical question is, how a flexural hinge can be designed to prevent fatigue failure, which is addressed in the second example.

6.2. Example 2: optimal design of a flexural hinge

Consider a parabolic flexural hinge undergoing superposed tensile ($F_x = 10 \pm 20$ N) and bending ($M_y = 120 \pm 50\,\mathrm{N\,mm^{-1}}$) cyclic loading. The monolithic CM is made of Al wrought alloy T351 and the flexural hinges are manufactured by drilling (surface roughness $R_t = 28$). The length l of the flexural hinge must be 1 mm so that it fits into the CM. The thinnest cross-section t_s and the notch depth t^* need to be determined in order to provide infinite life with safety factor $S_D \geq 2$ by performing the following steps:

1. Determine the surface roughness reduction factor by Fig. 6:

$$\gamma = 0.69.$$

2. Calculate the stress concentration factors by Eqs. (32) and (33):

$$\begin{aligned} K_{tt}^P = {} & 1 + (t^{*3} t_s^3 (2.t^* + t_s))^{0.5} * (0.01 t_s + 0.35 t^3 t_s^2 + 0.01 t^{*0.5} t_s^4 \\ & t^{*2} t_s (0.18 + 0.2 t_s^2) + t^* (0.02 + 0.09 t_s^2 + 0.01 t_s^4))^{-0.5}, \\ K_{tb}^P = {} & 1 + \left(0.32 t^{*1.32} + \frac{0.01 t_s}{t^{*2.66}(2t^* + t_s)} + \frac{0.02(1 + 4t^* t_s)^{2.25}}{(t^* t_s)^{3.38}} \right)^{-0.5}. \end{aligned}$$

3. Calculate the safety factor using Eq. (36):

$$S_D = \frac{2.05(1 + 5.28t^*)(K_{tt}^P - 485 t_s)(-72 K_{tb}^P + 485 t_s^2)}{t^* t_s (852,746 + 66,580.8 t_s) + K_{tb}^P (-2205 K_{tt}^P - 9884.16 t^* + 161,505 t_s) + K_{tt}^P (-1758.24 t^* + 12,610 t_s^2)}.$$

The dependencies between the design variables, t_s and t^*, and the safety factor S_D are illustrated in Fig. 7 for parabolic and circular flexural hinges. The latter one was obtained by a similar (but not explicitly shown) calculation. Geometric parameters can be chosen to achieve optimal flexural hinges with infinite life for a desired safety factor, e.g., $t^* = 3.5$ mm and $t_S = 1.0$ mm for $S_D = 2$.

7. Conclusions

In order to avoid fatigue failure of flexural hinges in compliant mechanisms, explicit analytical expressions for the fatigue life of rectangular, circular and parabolic flexural hinges were derived, accounting for stress concentration, surface finish and non-zero mean stresses. Time-harmonic, constant amplitude loads, namely axial forces, shear forces and bending moments, are considered. Optimally designed flexural hinges with an infinite life were then obtained by an inverse solution of the derived explicit expressions for given loads. Two example cases were described in detail to illustrate the proposed fatigue analysis and design process. Comparing circular and parabolic hinges in terms of fatigue life, it was shown, that circular hinges provide a "safer" design than parabolic hinges for a given thinnest cross-section. Or in other words, circular hinges can have a thinner cross-section than parabolic hinges, while providing the same safety against fatigue failure. From a topological synthesis standpoint, the derived, explicit, analytical expressions provide an effective analysis and design process, in order to incorporate optimal flexural hinges into compliant mechanisms for dynamic applications prior to any modelling or manufacturing efforts. This formulation eliminates unclear interpretation issues that would be encountered during any later manufacturing stage of a compliant mechanism.

Acknowledgements

This research was supported by priority programme grant SPP1476 from the German Research Foundation (DFG) and by a doctoral research stipend from the German Academic Exchange Service (DAAD-D/10/46834) to the first author.

References

[1] Ananthasuresh G, Kota S. Designing compliant mechanisms. Mechanical Engineering 1995;117:93–6 (New York, NY 1919).
[2] Frecker MI, Ananthasuresh GK, Nishiwaki S, Kikuchi N, Kota S. Topological synthesis of compliant mechanisms using multi-criteria optimization. Journal of Mechanical Design 1997;119:238–45.
[3] Saxena A, Ananthasuresh G. On an optimal property of compliant topologies. Structural and Multidisciplinary Optimization 2000;19:36–49.
[4] Howell L. Compliant mechanisms. New York: Wiley-Interscience; 2001.
[5] Bruns T, Tortorelli D. Topology optimization of non-linear elastic structures and compliant mechanisms. Computer Methods in Applied Mechanics and Engineering 2001;190:3443–59.
[6] Ansola R, Canales J, Tárrago J, Rasmussen J. An integrated approach for shape and topology optimization of shell structures. Computers and Structures 2002;80:449–58.

[7] Mattson C, Howell L, Magleby S. Development of commercially viable compliant mechanisms using the pseudo-rigid-body model: case studies of parallel mechanisms. Journal of Intelligent Material Systems and Structures 2004;15:195.
[8] Poulsen T. A simple scheme to prevent checkerboard patterns and one-node connected hinges in topology optimization. Structural and Multidisciplinary Optimization 2002;24:396–9.
[9] Paros J, Weisbord L. How to design flexural hinges. Machine Design 1965;25:151–6.
[10] Smith S. Flexures: elements of elastic mechanisms. CRC Press; 2000.
[11] Lobontiu N. Compliant mechanisms: design of flexure hinges. CRC Press; 2003.
[12] Tian Y, Shirinzadeh B, Zhang D. Closed-form compliance equations of filleted v-shaped flexure hinges for compliant mechanism design. Precision Engineering 2010;34:408–18.
[13] Lobontiu N, Paine J, OMalley E, Samuelson M. Parabolic and hyperbolic flexure hinges: flexibility, motion precision and stress characterization based on compliance closed-form equations. Precision Engineering 2002;26:183–92.
[14] Tian Y, Shirinzadeh B, Zhang D, Zhong Y. Three flexure hinges for compliant mechanism designs based on dimensionless graph analysis. Precision Engineering 2010;34:92–100.
[15] Dirksen F, Lammering R. On mechanical properties of planar flexure hinges of compliant mechanisms. Mechanical Sciences 2011;2:109–17 [special issue – Future directions in compliant mechanisms].
[16] Shuib S, Ridzwan M, Kadarman A, Perai S, Penang M. Methodology of compliant mechanisms and its current developments in applications: a review. American Journal of Applied Sciences 2007;4:160–7.
[17] Kaufman J. Properties of aluminum alloys: fatigue data and the effects of temperature, product form, and processing. Ohio: ASM Intl; 2008.
[18] Schijve J. Fatigue of structures and materials. Netherlands: Springer; 2001.
[19] Radaj D, Vormwald M. Ermüdungsfestigkeit: Grundlagen fur Ingenieure. Springer-Verlag; 2007.
[20] Gerber H. Bestimmung der zulassigen spannungen in eisenkonstruktionen. Zeitschrift des Bayerischen Architeckten und Ingenieur-Vereins 1874;6:101–10.
[21] Goodman J. Mechanics applied to engineering. London: Longman, Green and Co.; 1899.
[22] Soderberg C. Factor of safety and working stress. Transactions of ASME 1939;52:13–28.
[23] Suresh S. Fatigue of materials. Cambridge: Cambridge University Press; 1998.
[24] Pilkey D. Peterson's stress concentration factors. New Jersey: Wiley; 2008.
[25] Haibach E. Betriebsfestigkeit: Verfahren und Daten zur Bauteilberechnung. New York: Springer; 2006.
[26] Timoshenko S, Goodier J. Theory of elasticity. New York: McGraw-Hill; 1951.
[27] Issler L, Ruoß H, Häfele P. Festigkeitslehre – Grundlagen. 2nd ed. Berlin: Springer Verlag; 2005.
[28] Richtlinie, VDI, 2226, Empfehlung für die Festigkeitsberechnung metallischer Bauteile, VDI-Verlag GmbH Düsseldorf; 1965.
[29] Davim JP, editor. Surface integrity in machining. 1st ed. London: Springer; 2010.
[30] Service engineering bulletin sb021 – surface finish, http://www.engineaustralia.com.au/default/service_bulletin [accessed 15.11.11].